

# Applications of FDTD and FDM Algorithms for Cross-Verification of the Analyses of Hollow-Core Cylindrical Photonic Crystal Waveguides

**Jeong Kim**

*Department of Electric, Electronic and Communication Engineering Education,  
Chungnam National University, Daejeon, South Korea.*

## Abstract

Light-wave's propagation characteristics, governed by the physical laws of electrodynamic phenomena and described by Maxwell's equations, are investigated applying the finite-difference time-domain (FDTD) and finite difference method (FDM) approaches based on concrete mathematical foundation. As for novel waveguide design, hollow-core cylindrical photonic crystal waveguides are first proposed and analyzed by numerically solving coupled full-vectorially partial differential equations through derivational mathematics. Overall, results from FDTD and FDM agree very remarkably. The present detailed verification can provide a solid and reliable basis for further investigation in this research as well.

**Keywords:** Electrodynamic phenomena, FDTD, FDM, Effective refractive index

## 1. INTRODUCTION

In analogy to the basic concept that a spatial periodic arrangement of atoms or molecules constructs a normal crystal, it has been recently investigated that an artificial photonic crystal can be formed by modulating the relative refractive permittivity of a material with an appropriately-designed repeating pattern in space. Photonic crystal structures have received significant interest from researchers, who have found considerable innovative applications as in light-emitting diodes, lasers, optical fibers, nonlinear devices, and photovoltaic cells as a source of power for electronics [1-3]. As very special variant types of structures, low-index core photonic crystal fibers (PCFs) have been suggested, providing numerous advantages in terms of ultra-low flattened dispersion or effective material loss, high birefringence, very large effective area or power fraction, and sensing of the diverse liquids and gases [4-7].

Those promising photonic crystal structures have been analyzed by using simulation tools based on a finite element method with perfectly matched layer as the outer boundary layer. In this paper, hollow-core cylindrical photonic crystal waveguides (HCPCWs) are first proposed and analyses for the novel waveguide design have been innovatively performed, applying the finite-difference time-domain (FDTD) and finite difference method (FDM) approaches based on concrete mathematical foundation. Initially adopting the FDTD method to the proposed waveguides, the sequential electromagnetic field values in a finite volume of calculation space are sampled at equally spaced sampling points in time and at distinct points in a spatial lattice. The sampled data at the points are used for numerical calculations of allowed modes, without generating spurious mode solutions, in a given waveguide. Additionally, the FDM formulation can be obtained from the Helmholtz wave equation result. Employing the two numerical computation methods provides cross-verification and additive confidence in the accuracy of the results. In consecutive order, remarkable design of the HCPCW with reasonable guidance properties is addressed for device applications. This new type of numerical analysis and design approach can be reasonably expected to be useful in manufacturing processes and for fabrications of a variety of optical waveguide components.

## 2. MATHEMATICAL FORMULATIONS FOR THE FDTD AND FDM ALGORITHMS

An optically-guided lightwave is an electromagnetic vector field in nature, and thus its propagation characteristics are governed by the physical laws of electrodynamic phenomena which are collectively referred to as Maxwell's equations [8,9]. Maxwell's equations are the basis of the FDTD algorithm that can provide robust solutions and readily accommodate complex-valued material properties. An arbitrary material object can be approximated by building up computational unit cells for which field component positions are disposed with the desired values of electric permittivity ( $\epsilon$ ) and magnetic permeability ( $\mu$ ).

Founded on the MKS system of units, the full-vectorial curl differential form among Maxwell's four equations can be expressed by using partial derivatives as following:

$$\nabla \times \mathbf{H} = \left( \frac{\partial H_z}{\partial y} - \frac{\partial H_y}{\partial z} \right) \mathbf{a}_x + \left( \frac{\partial H_x}{\partial z} - \frac{\partial H_z}{\partial x} \right) \mathbf{a}_y + \left( \frac{\partial H_y}{\partial x} - \frac{\partial H_x}{\partial y} \right) \mathbf{a}_z = \epsilon \frac{d\mathbf{E}}{dt} \quad (1)$$

$$\nabla \times \mathbf{E} = \left( \frac{\partial E_z}{\partial y} - \frac{\partial E_y}{\partial z} \right) \mathbf{a}_x + \left( \frac{\partial E_x}{\partial z} - \frac{\partial E_z}{\partial x} \right) \mathbf{a}_y + \left( \frac{\partial E_y}{\partial x} - \frac{\partial E_x}{\partial y} \right) \mathbf{a}_z = -\mu \frac{d\mathbf{H}}{dt} \quad (2)$$

where the  $H_x$ ,  $H_y$ ,  $H_z$ ,  $E_x$ ,  $E_y$ , and  $E_z$  components of electromagnetic fields are inter-related in the rectangular coordinate system. Expanding the curl expressions and equating the like components, the system of six coupled partial differential equations

are formed for the FDTD analysis of electric and magnetic wave interactions with general three-dimensional (3D) objects [10].

Furthermore, these six equations are discretized in the space and time domains and formulated to find field solutions numerically [11,12], by assigning a calculation grid point in the rectangular lattice with digitized integers of k, l, m, and q as

$$\{k, l, m\} = \{k\Delta x, l\Delta y, m\Delta z\} \tag{3}$$

and any function of space and time as

$$f^q(k, l, m) = f(k\Delta x, l\Delta y, m\Delta z, q\Delta t) \tag{4}$$

where  $\Delta x$ ,  $\Delta y$ , and  $\Delta z$  are the lattice space increments in the x, y, and z coordinate directions, respectively, and  $\Delta t$  is the time increment [13]. By taking central finite difference approximation for space and time derivatives that are accurate to the second order [14], the partial derivatives are expressed as

$$\frac{\partial f^q(k, l, m)}{\partial x} = \frac{f^q\left(k + \frac{1}{2}, l, m\right) - f^q\left(k - \frac{1}{2}, l, m\right)}{\Delta x} + O(\Delta x^2) \tag{5}$$

$$\frac{\partial f^q(k, l, m)}{\partial t} = \frac{f^{\left(q+\frac{1}{2}\right)}(k, l, m) - f^{\left(q-\frac{1}{2}\right)}(k, l, m)}{\Delta t} + O(\Delta t^2) \tag{6}$$

Therefore, by applying logical and robust algorithms further in the cross section for the proposed waveguide and adopting the central finite-difference space and time expressions with accuracy to the second order, the following relationships as representative cases in a 3D FDTD formulation can be developed:

$$H_x^{q+\frac{1}{2}}\left(k, l + \frac{1}{2}, m + \frac{1}{2}\right) = H_x^{q-\frac{1}{2}}\left(k, l + \frac{1}{2}, m + \frac{1}{2}\right) + \frac{\Delta t}{\mu} \left\{ \left[ \frac{E_y^q\left(k, l + \frac{1}{2}, m + 1\right) - E_y^q\left(k, l + \frac{1}{2}, m\right)}{\Delta z} \right] - \left[ \frac{E_z^q\left(k, l + 1, m + \frac{1}{2}\right) - E_z^q\left(k, l, m + \frac{1}{2}\right)}{\Delta y} \right] \right\} \tag{7}$$

$$E_z^{q+1}\left(k, l, m + \frac{1}{2}\right) = E_z^q\left(k, l, m + \frac{1}{2}\right) + \frac{\Delta t}{\varepsilon\left(k, l, m + \frac{1}{2}\right)} \left\{ \left[ \frac{H_y^{q+\frac{1}{2}}\left(k + \frac{1}{2}, l, m + \frac{1}{2}\right) - H_y^{q+\frac{1}{2}}\left(k - \frac{1}{2}, l, m + \frac{1}{2}\right)}{\Delta x} \right] - \left[ \frac{H_x^{q+\frac{1}{2}}\left(k, l + \frac{1}{2}, m + \frac{1}{2}\right) - H_x^{q+\frac{1}{2}}\left(k, l - \frac{1}{2}, m + \frac{1}{2}\right)}{\Delta y} \right] \right\} \tag{8}$$

By using phasor notation with the axial propagation constant ( $\beta$ ), the first-order partial derivatives with respect to  $z$  are replaced with  $-j\beta$ , because variations of material properties are normally limited to the transverse directions and the  $z$ -dependence of fields is as  $\exp(-j\beta z)$ . And two adjacent fields required for the first-order derivatives in the discretized space region can be represented by a field at the middle point between them. Hence, the following equations related to expressions (7) and (8), respectively, can be formulated:

$$H_x^{q+\frac{1}{2}}(k, l+\frac{1}{2}) = H_x^{q-\frac{1}{2}}(k, l+\frac{1}{2}) + \frac{\Delta t}{\mu} \left\{ -j\beta \cdot E_y^q(k, l+\frac{1}{2}) - \left[ \frac{E_z^q(k, l+1) - E_z^q(k, l)}{\Delta y} \right] \right\} \quad (9)$$

$$E_z^{q+1}(k, l) = E_z^q(k, l) + \frac{\Delta t}{\varepsilon_0 \varepsilon_r(k, l)} \left\{ \left[ \frac{H_y^{q+\frac{1}{2}}(k+\frac{1}{2}, l) - H_y^{q+\frac{1}{2}}(k-\frac{1}{2}, l)}{\Delta x} \right] - \left[ \frac{H_x^{q+\frac{1}{2}}(k, l+\frac{1}{2}) - H_x^{q+\frac{1}{2}}(k, l-\frac{1}{2})}{\Delta y} \right] \right\} \quad (10)$$

Moreover, in modeling regions extending to infinity with this efficient algorithm, a perfectly matched layer (PML) to make a highly absorbing boundary condition satisfied is effectively designed at the outer material boundary of a computation domain. Ideally, the absorbing medium is only as thick as a few lattice cells, highly absorbing, reflectionless to all impinging electromagnetic waves, and effective over the full range of operating wavelengths.

As in the development of the FDTD algorithm, the FDM formulation can be derived from the coupled Maxwell's equations [11]. For continuous waves in linear and isotropic media, combining equations (1) and (2) results in the following vectorial wave expression:

$$\nabla \times \nabla \times \mathbf{E} - n_r^2 k_0^2 \mathbf{E} = 0 \quad (11)$$

where  $n_r$  is the refractive index and  $k_0$  is the propagation constant in free space. Many waveguiding devices, like optical fibers, can be viewed as  $z$ -invariant, or piecewise  $z$ -invariant structures. For those structures, the refractive index  $n_r(x, y, z)$  varies slowly along the propagation direction  $z$ , which is valid for most photonic guided-wave devices. By using the vector identity of  $\nabla \times \nabla \times = \nabla(\nabla \cdot) - \nabla^2$ , equation (11) can be written as the following Helmholtz wave form:

$$\nabla^2 \mathbf{E} + n_r^2 k_0^2 \mathbf{E} = \nabla(\nabla \cdot \mathbf{E}) \quad (12)$$

Also with the reasonable assumption of negligible time dependency along the  $z$ -axis, the FDM formulation as in equation (12) can be implemented by replacing spatial

derivatives with finite difference approximations. Here, it is noted that the transverse component of (12) is

$$\nabla^2 \mathbf{E}_t + n_r^2 k_0^2 \mathbf{E}_t = \nabla_t \left( \nabla_t \cdot \mathbf{E}_t + \frac{\partial E_z}{\partial z} \right) \tag{13}$$

where the subscript “t” stands for the transverse components. Consequently, by applying both the developed digital calculation algorithms, complicated structures such as the proposed HCPCWs can be exploited to yield the propagation characteristics.

### 3. DESIGN AND ANALYSIS OF THE PROPOSED HCPCW

Since cylindrically-modulating PCWs have periodic index variations in the radial direction only, a low-index core PCW with  $N = 15$  layers as in Figure 1(a) consists of  $r_1 = 0.6 \mu\text{m}$  and  $r_2 = 1.2 \mu\text{m}$ , forming a low-index core, located in the core region with a variable radius of  $r_1$  and surrounded by a clad region composed of alternating-index and equal-thickness rings with  $d_a = 0.2 \mu\text{m}$  and  $d_g = 0.3 \mu\text{m}$  for the primary design. Here,  $d_a$  and  $d_g$  in the refractive index profile for the proposed geometry denote thicknesses of air and pure-silica glass layers [15], respectively. Because of the periodic index profiles, either a high (silica glass) refractive index ( $n_1$ ) or a low (air) refractive index ( $n_0$ ) is employed for the  $n_r$  value. One such light-guiding fiber is composed of  $N$  linear, isotropic, homogeneous and cylindrically symmetric dielectric layers as illustrated in Figure 1(b).

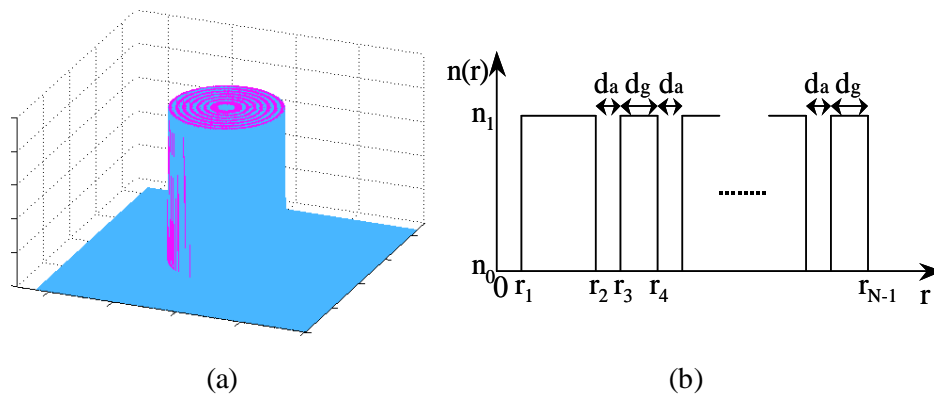


**Figure 1.** Schematics of a proposed HCPCW with an air core by (a) the three-dimensional view and (b) the refractive index profile

When assuming the glass portion of the designed waveguide has a refractive index of 1.45 with no material dispersion, the FDTD method is an efficient approach for calculation of the normalized propagation constants of guided modes. In order to find

the effective refractive index ( $\bar{\beta}$ ) variation, a reasonable  $\beta$  value also needs to be chosen. Therefore, the operation wavelength ( $\lambda$ ) associated with the  $\beta$  value of the fundamental mode can be calculated.

By generating the source of an impulse function in the time domain covering an infinite spectrum, the proposed waveguide can be excited. Figure 2 depicts spectral data for different  $\beta$  values for the proposed HCPCW with  $r_1 = 0.6 \mu\text{m}$ ,  $r_2 = 1.2 \mu\text{m}$ ,  $d_a = 0.2 \mu\text{m}$ ,  $d_g = 0.3 \mu\text{m}$ , and a total of fifteen layers.

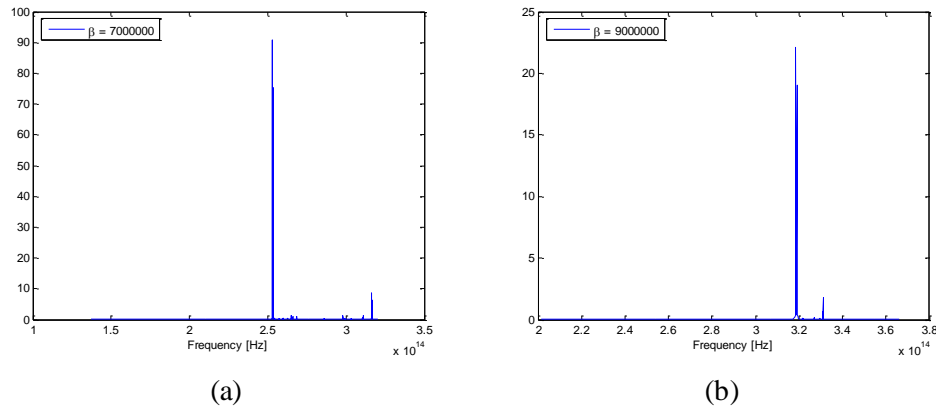


**Figure 2.** Spectrum for the proposed HCPCW with  $r_1 = 0.6 \mu\text{m}$ ,  $r_2 = 1.2 \mu\text{m}$ ,  $d_a = 0.2 \mu\text{m}$ ,  $d_g = 0.3 \mu\text{m}$ , and  $N = 15$ , when (a)  $\beta = 7,000,000$  and (b)  $\beta = 9,000,000$

Once spectral data for different  $\beta$  values are digitally-computed, mode index results as a function of normalized wavelengths can be calculated. For example, when  $\beta = 7,000,000$  as in Figure 2(a), the normalized propagation constant can be found to be about 1.32078 by using the peak frequency ( $f_p$ ) value of  $2.531 \times 10^{14}$  Hz as follows [12]:

$$\bar{\beta} = \frac{\beta c_0}{2\pi f_p} = \frac{7000000}{2\pi} \frac{3.0 \times 10^8}{2.53052 \times 10^{14}} \approx 1.32078 \quad (14)$$

where  $c_0$  is equal to the speed of light in free space. Figure 3 illustrates spectral data for the HCPCW designed with  $r_1 = 0.4 \mu\text{m}$ ,  $r_2 = 1.2 \mu\text{m}$ ,  $d_a = 0.2 \mu\text{m}$ ,  $d_g = 0.3 \mu\text{m}$ , and fifteen layers. As noticed, more apparent sharp peak frequency can be evidently found at  $2.465 \times 10^{14}$  Hz for  $\beta = 7,000,000$ .

Similarly to the FDTD method based on mathematical foundation, the FDM algorithm is reasonably applied to the numerical calculation of propagation characteristics such as effective refractive index [9]. As an initial investigation, complicated structures of the same proposed HCPCWs are exploited to yield the normalized propagation

constants, which are compared with the results from the FDTD algorithm. Figure 4 illustrates the effective refractive index versus the operation wavelength for the fundamental mode without taking into account the material dispersion effect [12].

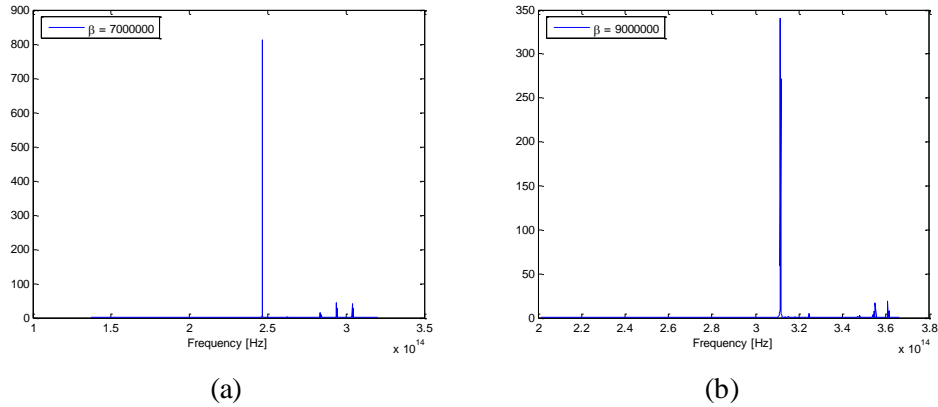


**Figure 3.** Spectrum for the proposed HCPCW with  $r_1 = 0.4 \mu\text{m}$ ,  $r_2 = 1.2 \mu\text{m}$ ,  $d_a = 0.2 \mu\text{m}$ ,  $d_g = 0.3 \mu\text{m}$ , and  $N = 15$ , when (a)  $\beta = 7,000,000$  and (b)  $\beta = 9,000,000$

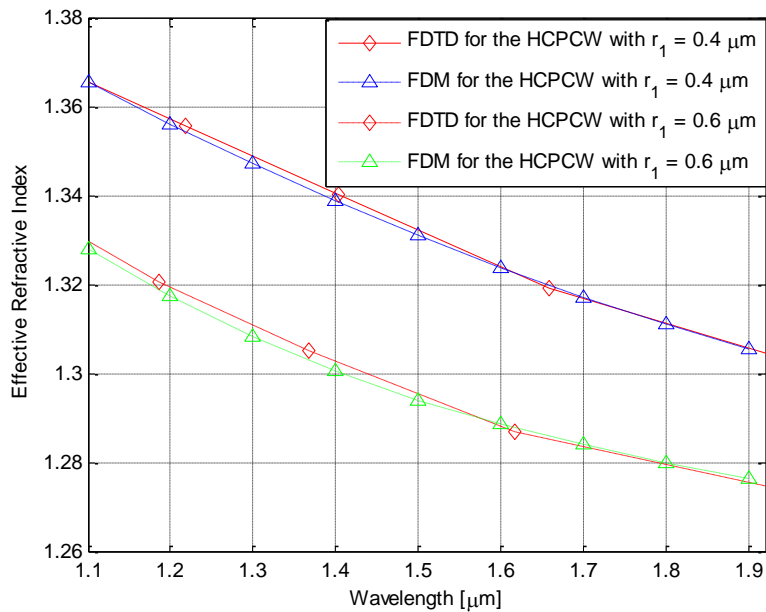


**Figure 4.** Variations of the effective refractive index versus the operation wavelength for the HCPCW with  $r_1 = 0.4 \mu\text{m}$  or  $r_1 = 0.6 \mu\text{m}$ , and a total of 15 layers

As clearly noticed in Figure 4 for the HCPCW designed with  $r_1 = 0.4 \mu\text{m}$ ,  $r_2 = 1.2 \mu\text{m}$ ,  $d_a = 0.2 \mu\text{m}$ ,  $d_g = 0.3 \mu\text{m}$ , and a total of 15 layers, results from FDTD and FDM, which are denoted by the solid red line with the diamond symbol and the dashed blue

line with the up-triangle symbol, respectively, agree very well. When operating the proposed HCPCW at the wavelength of around 1.4  $\mu\text{m}$ , the FDTD analysis produces the effective refractive index of 1.3406. Meanwhile, the FDM technique yields the  $\bar{\beta}$  value of 1.3392 about the same operation wavelength. Almost negligible difference of 0.0014 is noticed. Overall, agreements are remarkable. Also based on the obviously strongest clear peak in each spectrum in Figure 3(a) for  $\beta = 7,000,000$  and Figure 3(b) for  $\beta = 9,000,000$ , the effective refractive indices are computed to be about 1.3561, and 1.3801 at the operating wavelengths of 1.2172, and 0.9635, respectively.

Again for the HCPCW designed with  $r_1 = 0.6 \mu\text{m}$ ,  $r_2 = 1.2 \mu\text{m}$ ,  $d_a = 0.2 \mu\text{m}$ ,  $d_g = 0.3 \mu\text{m}$ , and a total of 15 layers, it is noticed that the  $\bar{\beta}$  value results from FDTD and FDM, which are denoted by the dashed red curve with the diamond symbol and the dotted green curve with the triangle symbol, respectively, also agree well as for the same HCPCW in Figure 4. Here, it is reasonably observed that, since one sharp distinct spike exists in each spectrum in Figure 2(a) for  $\beta = 7,000,000$  and Figure 2(b) for  $\beta = 9,000,000$ , there is strong single-mode operation through the operation wavelength from 1.1 to 1.9  $\mu\text{m}$ , which is remarkably optimistic for realistic communication or optical sensor applications.

In the same way as the elementary fundamental evaluation approaches, based on FDTD and FDM algorithms, are cross-verified, the overall light-guiding operation tendency can be analyzed numerically. The present detailed verification can provide a solid and reliable basis for further investigation in this research as well.

#### 4. CONCLUSION

The mathematical derivation has been preceded and the algorithm addressed for the FDTD and FDM approaches to find out the propagation characteristics of optical waveguides. Expanding the curl expressions of full-vectorial Maxwell's equations with the first-order derivatives and equating the like components, the system of six coupled partial differential equations are formed for the FDTD analysis of electric and magnetic wave interactions with the proposed HCPCWs. By taking central finite difference approximation for space and time derivatives that are accurate to the second order, the sequential electromagnetic field values in a finite volume of calculation space are sampled at equally spaced sampling points in time and at distinct points in a spatial lattice. The sampled data at the points are used for the numerical calculations of allowed modes. Likewise, the FDM formulation can be obtained from the Helmholtz wave equation result and implemented by replacing spatial derivatives with finite difference forms.

For the proposed HCPCW with  $r_1 = 0.4 \mu\text{m}$  or  $r_1 = 0.6 \mu\text{m}$ ,  $r_2 = 1.2 \mu\text{m}$ ,  $d_a = 0.2 \mu\text{m}$ ,  $d_g = 0.3 \mu\text{m}$ , and a total of 15 layers, overall agreements by effective refractive index results from FDTD and FDM algorithms are remarkable through the operation wavelength from 1.1 to 1.9  $\mu\text{m}$ . In the same way as the elementary fundamental evaluation approaches, based on FDTD and FDM algorithms, are cross-verified, the overall light-guiding operation tendency can be analyzed numerically. The present

detailed verification can provide a solid and reliable basis for further investigation in this research as well.

## REFERENCES

- [1] Hwang, D.-K., Lee, B., and Kim, D.-H., 2013, "Efficiency Enhancement in Solid Dye-Sensitized Solar Cell by Three-Dimensional Photonic Crystal," *RSC Advances*, **3.9**, pp. 3017-3023.
- [2] Rifat, A. A., Ahmed, K., Asaduzzaman, S., Paul, B. K., and Ahmed, R., 2019, *Development of Photonic Crystal Fiber-Based Gas/Chemical Sensors, Computational Photonic Sensors*, Springer Nature, Switzerland.
- [3] Islam, Md. S., Sultana, J., Dinovitser, A., Ahmed, K., Ng, B. W.-H., and Abbott, D., 2018, "Sensing of Toxic Chemicals Using Polarized Photonic Crystal Fiber in the Terahertz Regime," *Optics Communications*, **426**, pp. 341-347.
- [4] Zhang, Y., Jing, X., Qiao, D., and Xue, L., 2020, "Photonic-Crystal Fiber with Ultra-Low Flattened Dispersion and High Birefringence for Terahertz Transmission," *Frontiers in Physics*, **8**, p. 370.
- [5] Sardar, Md. R., Faisal, M., and Ahmed, K., 2021, "Simple Hollow Core Photonic Crystal Fiber for Monitoring Carbon Dioxide Gas with Very High Accuracy," *Sensing and Bio-Sensing Research*, **31**, p. 100401.
- [6] Rahman, Md. M., Mou, F. A., Bhuiyan, M. I. H., and Islam, M. R., 2020, "Design and Characterization of a Circular Sector Core Cladding Structured Photonic Crystal Fiber with Ultra-Low EML and Flattened Dispersion in the THz Regime," *Optical Fiber Technology*, **55**, p. 102158.
- [7] Maida, A. M., Abas, P. E., Petra, P. I., Kaijage, S., Zou, N., and Begum, F., 2021, "Theoretical Considerations of Photonic Crystal Fiber with All Uniform-Sized Air Holes for Liquid Sensing," *Photonics*, **8**, p. 249.
- [8] Balanis, C. A., 1989, *Advanced Engineering Electromagnetics*, Wiley, New York.
- [9] Kim, J., 2012, "Effects of Core and Cladding on Optical Guidance Properties of Holey Fibers," *Optical Communication*, InTech, Croatia, pp. 25-40.
- [10] Taflove, A. and Hagness, S. C., 2005, *Computational Electrodynamics: the Finite-Difference Time-Domain Method*, Artech House, Boston.
- [11] Hayt, W. H. Jr. and Buck, J. A., 2019, *Engineering Electromagnetics*, McGraw Hill, New York.
- [12] Keiser, G., 2000, *Optical Fiber Communications*, McGraw Hill, New York.
- [13] Kunz, K. S. and Luebbers, R. J., 1993, *The Finite Difference Time Domain Method for Electromagnetics*, CRC Press, Boca Raton.

- [14] Kreyszig, E., 2011, *Advanced Engineering Mathematics*, Wiley, New Jersey.
- [15] Agrawal, G. P., 2001, *Nonlinear Fiber Optics*, Academic Press, San Diego.